Chapter 6
The Retinal TNAP

Orsolya Kántor, Dorottya Cserpán, Béla Völgyi, Ákos Lukáts and Zoltán Somogyvári

Abstract Accumulating evidence from recent literature underline the important roles of tissue non specific alkaline phosphatase (TNAP) in diverse functions as well as diseases of the nervous system. Exploration of TNAP in well characterized neural circuits such as the retina, might significantly advance our understanding regarding neural TNAP's roles. This chapter reviews the scarce literature as well as our findings on retinal TNAP. We found that retinal TNAP activity was preserved and followed diverse patterns throughout vertebrate evolution. We have consistently observed TNAP activity (1) in retinal vessels, (2) in photoreceptors and (3) in the majority of the studied species in the outer (OPL) and inner plexiform layers (IPL), where synaptic transmission occurs. Importantly, in some species the IPL exhibits several TNAP positive strata. These strata exactly corresponded those seen after quadruple immunohistochemistry with four canonical IPL markers (tyrosine hydroxylase, choline acetyltransferase, calretinin, protein kinase C α). Diabetes results in diminishing retinal TNAP activity before changes in canonical markers

O. Kántor (✉)
Department of Anatomy, Histology and Embryology, Semmelweis University, Tűzoltó str. 58, Budapest 1094, Hungary
e-mail: kantor.orsolya@med.semmelweis-univ.hu

D. Cserpán · Z. Somogyvári
Theoretical Neuroscience and Complex Systems Research Group, Wigner Research Center for Physics, Hungarian Academy of Sciences, Budapest, Hungary

B. Völgyi
Department of Experimental Zoology and Neurobiology, University of Pécs, Pécs, Hungary

B. Völgyi
János Szentágothai Research Center, Pécs, Hungary

Á. Lukáts
Department of Human Morphology and Developmental Biology, Semmelweis University, Budapest, Hungary

C. Fonta and L. Négyessy (eds.), *Neuronal Tissue-Nonspecific Alkaline Phosphatase (TNAP)*, Subcellular Biochemistry 76,
DOI 10.1007/978-94-017-7197-9_6

could be observed in a rat model. The presence of TNAP activity at critical sites of neurotransmission suggests its important and evolutionary conserved role in vision. In diabetes, the decreased TNAP activity indicates neurological alterations adding further evidence for the role of TNAP in brain diseases.

Keywords TNAP · Retina · Inner plexiform layer · Visual processing · Diabetes

6.1 Brief Introduction to the Retina

The retina, which is part of the diencephalon, lies outside the brain and is connected through the optic nerve to it. In the mammalian retina approximately 50–60 different cell types serve the detection and initial processing of light impulses. With the exception of primate fovea, these cell types are distributed in a fairly even way, consisting of many parallel, anatomically equipotent microcircuits rather than of a few major pathways. Elaborate chemical as well as electrical synapses enable communication between the neurons. Schematized, information flows through vertical channels between photoreceptors, bipolars and ganglion cells (the sole retinal output neurons). This information flow is modified in the lateral direction through horizontal and amacrine cells. The diverse cell types are arranged in a crystallised anatomical structure. Photosensitive elements, cell bodies and interconnected fibers of the retinal neurons are strictly organized in nine neuronal layers: (1) photoreceptor layer (photosensitive parts of rods and cones), (2) outer limiting membrane (consisting of the outer processes of Müller glia), (3) inner nuclear layer (INL, cell bodies of rods and cones), (4) outer plexiform layer (OPL, highly specialized synapses between rods, cones and bipolar and horizontal cells), (5) inner nuclear layer (INL, cell bodies of horizontal, bipolar and amacrine cells as well as Müller glia), (6) inner plexiform layer (IPL, an ordered stack of synaptic planes between bipolars, amacrines and ganglion cells), (7) ganglion cell layer (GCL, cell bodies of ganglion cells), (8) nerve fiber layer (composed of the axons of ganglion cells running toward the optic disk), (9) inner limiting membrane (inner fibers of the Müller glia isolating the neural retina from the vitreous body). As compared to other parts of the central nervous system, retinal cell types and their connections are fairly well characterized. Well known connections, easy accessibility and stimulability of the neurons render the retina a widely used model system in neuroscience research.

Moreover, common systemic human diseases (most frequently hypertension and diabetes mellitus) can result in severe ocular complications leading (if untreated) often to blindness. The retina is the only part of the organism where arterioles (affected by the above diseases) can be observed directly as part of ophthalmological examination. Other common neurological diseases such as Alzheimer's and Parkinson's disease (see recent reviews Dehabadi et al. 2014; Bodis-Wollner et al. 2014) also have ocular manifestations, therefore, retinal research has a major impact also on human pathophysiology.

Although research tackling TNAP's involvement in functioning and malfunctioning of the nervous system is emerging, little attention was paid on the retina. In this chapter we summarize the sparse literature and our findings in this field.

6.2 Localisation of Retinal TNAP Activity in Different Mammalian and Non-Mammalian Species

TNAP activity was reported in the homogenized retina of chicken embryos as early as 1949 (Lindeman 1949) and on histological sections in 1963 (Rogers 1963). In mammals, a few controversial papers exist, which were debated even at their time because of unreliability of the used histochemical methods (Yoshida 1957; De Vincentiis and Testa 1959; Reis 1954). Although the reliable diazo-dye method was used in the work of Reis (1954) in ox, the paper was focused on retinal vessels instead of neural-glial elements. More recently, Iandiev et al. (2007) found no detectable TNAP activity in mouse retina. However, in their work the histochemical reaction was carried out at pH 7.4 which lies well under the pH optimum of alkaline phosphatase (pH 9.3; Fedde and Whyte 1990).

In our very recent work (Kántor et al. 2014), we investigated the presence and pattern of TNAP activity in the retinas of several species throughout the vertebral evolution: in zebrafish, convict cichlid, frog, chicken, rat, mice, rabbit, golden hamster, guinea pig, ferret, cat, dog, squirrel monkey. Additionally, post-mortem samples from human patients without reported eye disease were also investigated. Western blot (WB) analysis and TNAP enzyme histochemistry were carried out on the samples.

In the studied species, polyclonal rabbit TNAP antibody (1:2,000; Abcam, ab65834, Cambridge, UK; Díaz-Hernandez et al. 2010) detected a single band of approximately 90 kDa in the samples (Fig. 6.1), which corresponds to the molecular weight of TNAP dimer (NCBI Protein Database, Le Du and Millán 2002). Therefore, TNAP is expressed in the retina of a wide range of vertebrate species.

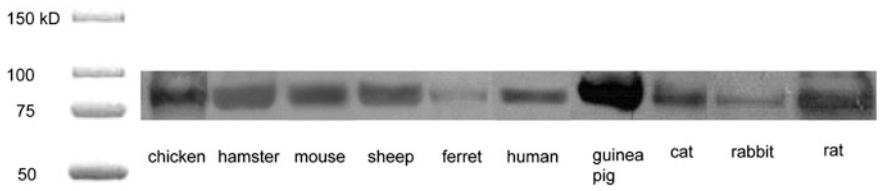

Fig. 6.1 Western blot analysis of TNAP in retinas of different species. A single band at 90 kDa was detected in each investigated species. *Left* molecular marker. Originally published in Cell and Tissue Research, vol. 358, p. 90, Fig. 6.1, TNAP activity is localized at critical sites of retinal neurotransmission across various vertebrate species, Kántor O, Varga A, Kovács-Öller T, Énzsöly A, Balogh L, Baksa G, Szepessy Z, Fonta C, Roe AW, Nitschke R, Szél Á, Négyessy L, Völgyi B, Lukáts Á. With kind permission from Springer Science and Business media

The strength of the TNAP bands varied across the different species, suggesting a difference in the expression levels.

After TNAP histochemistry, a tremendous variation of TNAP activity patterns were found in retinal sections of the examined species. The species were grouped according to their activity pattern and representative species are shown in Fig. 6.2.

6.2.1 All or None: Dog, Zebrafish

In the dog retina, no neural elements, only retinal vessels showed alkaline phosphatase activity (asterisks on Fig. 6.2a). Lutty and McLeod (2005) reported similar findings. In contrast, TNAP activity was present in all layers of the zebrafish retina (Fig. 6.2b). Somata in the nuclear layers as well as both plexiform layers were extensively outlined by the reaction product. Notably, four darkly and three intermingled relatively lightly stained strata of the inner plexiform layer (IPL) became visible. In the photoreceptors' layer, the triangular shaped outer segments of short single cones (arrows) were heavily, whereas long single cone, double cone and rod outer segments only weakly stained.

Retinal TNAP activity pattern in sheep and cichlid fish (not shown) was similar to that of the zebrafish, except that no stratification pattern of the IPL was found after the histochemical reaction.

6.2.2 TNAP Activity in the Outer Retina: Squirrel Monkey and Ferret

We found a pronounced difference between the staining intensity of the outer and inner retina of the squirrel monkey (Fig. 6.2c) and ferret (not shown). In both species, inner retinas remained unstained, whereas considerable TNAP activity was detected in the outer retinas. In the photoreceptor layer, rod outer segments displayed moderate TNAP activity, whereas their inner segments were relatively heavily labeled. In contrast, cone inner segments (arrows on Fig. 6.2c) displayed lower activity than the surrounding rod inner segments, thus seeming to be TNAP negative. Somata of photoreceptors in the outer nuclear layer were homogenously delineated by moderate enzymatic activity that rapidly declined from the OPL inward and resulted in very weak or no staining in the inner retina. Beside neuronal elements, blood vessels also displayed TNAP activity in the squirrel monkey and ferret.

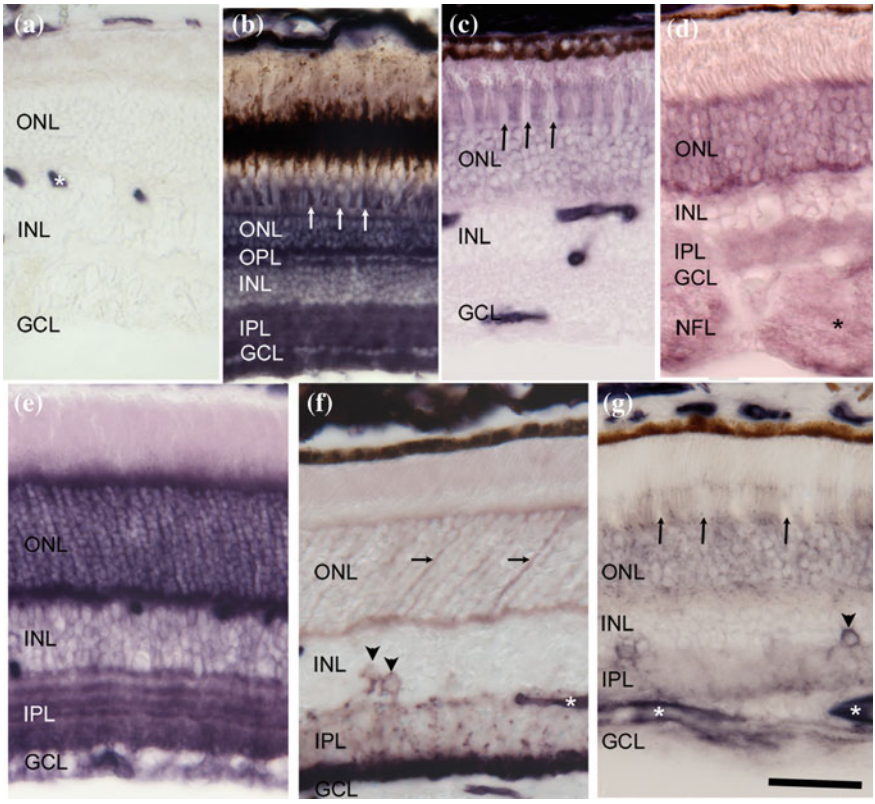

Fig. 6.2 Representative species showing different patterns of retinal TNAP activity. In dog (**a**), only retinal vessels (*asterisk*) displayed TNAP activity. In contrast, in zebrafish (**b**), all retinal layers were strongly stained. *Arrows* single short cones. In squirrel monkey (**c**), only the outer retina showed TNAP staining, cones (*arrows*) were much more weakly stained than the surrounding rod inner segments. OPL showed moderate TNAP activity, whereas the intensity of the staining dropped abruptly towards the inner retina. In rabbit (**d**), photoreceptor inner segments, somata and both plexiform layers were heavily stained. Moreover, at central locations, bundles of optic fibers (*asterisk*) also displayed moderate TNAP activity. In rat (**e**), TNAP activity was most prominent at the level of the outer segments, in the OPL and ONL. Moreover, in the IPL, five darkly labeled strata and a fainter stained stripe with intervened lighter strata became visible. In mice (**f**), photoreceptors were moderately, somata strongly stained. Occasionaly, some photoreceptors (*cones*, *arrows*) could be traced until their end feet embedded in the heavily stained OPL. Some amacrine cells (*arrowheads*) in the INL were also outstandingly labeled, with processes ending in the innermost stratum of the IPL. In contrast, in the human retina (**g**), inner segments of cones (*arrows*) were more weakly stained than surrounding rods. In the INL, some amacrine cells (*arrowheads*) were also heavily stained with processes ending also in the innermost layer of the IPL. *ONL* outer nuclear layer, *INL* inner nuclear layer, *GCL* ganglion cell layer, *OPL* outer plexiform layer, *IPL* inner plexiform layer, *NFL* nerve fiber layer. *Bar* 50 µm. Parts of the figure are originally published in Cell and Tissue Research, vol. 358, Fig. 3b, 4a, 5b, 8e, pp. 91, 92 and 96, respectively. TNAP activity is localized at critical sites of retinal neurotransmission across various vertebrate species, Kántor O, Varga A, Kovács-Öller T, Énzsöly A, Balogh L, Baksa G, Szepessy Z, Fonta C, Roe AW, Nitschke R, Szél Á, Négyessy L, Völgyi B, Lukáts Á. With kind permission from Springer Science and Business media

6.2.3 TNAP Activity in the Photoreceptor and Synaptic Layers: Cat, Rabbit and Guinea Pig

In rabbit, blood vessels are only present in the optic disc area and, as in previous species, they showed TNAP activity (picture not shown). Rod inner segments, photoreceptor somata and terminals became visible after TNAP histochemistry. The strongest TNAP activity was found at the level of rod outer segments and in the OPL. The IPL and (at central locations) bundles of optic fibers (asteriks on Fig. 6.2d) were moderately stained.

In cat and guinea pig the TNAP staining pattern was similar to that of the rabbit. Interestingly, in guinea pig, TNAP histochemistry revealed three darkly labeled strata in the IPL. Moreover, some amacrine cells were also outlined by the purple reaction product.

6.2.4 *TNAP Activity in Multiple Strata of the IPL: Rat and Chicken*

In the retina of all investigated rat strains (Sprague-Dawley, Wistar and Long Evans), blood vessels were darkly stained by TNAP enzyme histochemistry (Fig. 6.2e). Weak, homogenous TNAP staining was seen at the level of the outer segments, whereas the activity was more intense in the layer of the inner segments. Somata in the outer nuclear layer as well as photoreceptor terminals in the OPL were densely stained. Soma outlines in both the INL and GCL and the entire IPL displayed TNAP activity. TNAP histochemistry revealed five dark and one somewhat fainter TNAP positive layers in the IPL that were separated by thin TNAP negative stripes. The detailed description of the exact position of these strata is given in the following section.

In the adult chicken retina (picture not shown), similarly to rats, photoreceptors (especially inner segments) and both plexiform layers displayed strong TNAP activity. As seen in rats, several strata in the IPL became visible after TNAP histochemistry. Moreover, calretinin containing horizontal cells were also heavily stained. In central retinal locations, where the optic fiber layer is prominent, TNAP-labeled optic axons became visible.

6.2.5 *TNAP Positivity in Retinal Amacrine Cells: Frog, Mouse, Golden Hamster and Human*

Blood vessels were strongly TNAP stained in the mouse retina (asterisk on Fig. 6.2f). A moderate enzymatic activity was found in the photoreceptor layer. Here, outer segments displayed stronger staining than the inner segments.

Occasionally, cell bodies and photoreceptor inner fibers exhibited strong TNAP labeling (arrows on Fig. 6.2f). In these latter cases the TNAP stained photoreceptors were traceable to their pedicles embedded in the less prominently stained OPL. In the inner retina, a subpopulation of amacrine cells displayed marked TNAP activity (arrowheads on Fig. 6.2f). Their fine processes were apparent as they richly arborized in the IPL. Most of these TNAP labeled amacrine cell processes ended in the innermost strata of the IPL (Fig. 6.2f), where the strongest TNAP labeling was seen. In these subset of amacrine cells, TNAP activity colocalized with glutamic acid decarboxylase (GAD67) immunoreactivity showing that they corresponded to to GABAergic amacrine cells.

TNAP labeling in golden hamster (picture not shown) was similar to the pattern seen in mice. Interestingly, this was the only species where vessels displayed no detectable TNAP activity.

In the human retina, blood vessels exhibited a strong TNAP labeling (asterisks on Fig. 6.2g). Rod photoreceptor outer segments were only lightly stained, whereas a somewhat stronger TNAP labeling was seen at the level of the inner segments. Interestingly, both cone outer and inner segments (arrows on Fig. 6.2g) were much weaker (if at all) TNAP stained. Photoreceptor somata were clearly outlined by the TNAP reaction product while the staining intensity was only moderate in the OPL. In the inner retina, some amacrine cells became visible by the TNAP staining (arrowhead on Fig. 6.2g). Occasionally, dendritic processes of these amacrine cells were apparent as they entered the inner division of the IPL. As seen in mouse and hamster, the dendrites of these amacrine cells reached the innermost stratum of the IPL. Here, TNAP activity appeared to be somewhat stronger than in the outer parts of the layer.

TNAP staining pattern in the frog retina (data not shown) was similar to the other species in this subgroup. The IPL was divided into seven strata by three strongly and four weakly TNAP stained stripes.

In summary, retinal TNAP activity was retained throughout vertebrate evolution. The activity pattern in the examined species differed tremendously. However, some trends were found regarding the TNAP staining pattern. (1) Retinal blood vessels displayed strong TNAP activity in all examined species but the golden hamster. (2) Photoreceptors were consistenty stained, however, the staining was not constricted to either rods or cones. (3) In the majority of the examined species, OPL and IPL, layers where synaptic connections occur were also TNAP labeled. We do not have direct electron microscopical evidence but this latter finding suggests that, similarly to the vertebrate neocortex (Fonta et al. 2004; Négyessy et al. 2011), retinal TNAP activity also plays a role in synaptic functions. 4 In some studied species, the inner retina also displayed TNAP activity. In certain species (frog, guinea pig, mice, golden hamster, human) some amacrine cells were outlined by the TNAP staining, in other species (zebrafish, chicken, rat, mice, golden hamster, human) strata of the IPL were revealed by TNAP histochemistry. The variations of the staining patterns did not follow evolutionary relationships, as evolutionary distant species (e.g. frog and humans) displayed similar patterns, whereas closely related species (e.g. squirrel monkey and humans) were often different. The staining

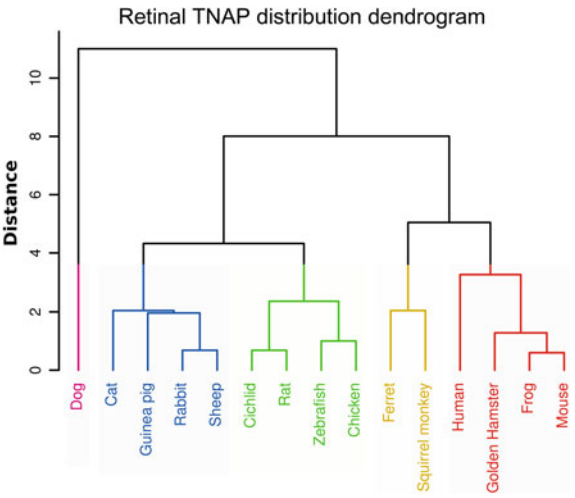

Fig. 6.3 Hierarchical clustering of the retinal TNAP distribution of the examined species resulted in five main clusters of species depicted by different colors

pattern did not vary according to the diurnal life style of the species, since crepuscular dog, cat and rodents showed great differences. The real cause of the described variations remains obscure.

In order to examine the structural similarities between retinal TNAP distribution among the examined species in an observer independent manner, we performed hierarchical cluster analysis on the retinal layer staining intensity profiles. The I_j layer staining intensities were described semiquantitatively on a 0–3 scale. The distance between the staining intensity profiles were measured as:

$$D_{jk} = \mathrm{sum}\left(\mathrm{abs}\left(I_j^{0.75} - I_k^{0.75}\right)\right)$$

Then, the complete linkage hierarchical clustering algorithm were performed in R (http://cran.r-project.org), in which we merge in each step the two clusters with the smallest maximum pairwise distance. The resulted similarity tree is presented as a dendrogram on Fig. 6.3, where the 5 main branches are colored to emphasize the structural families. The resulting clusters of species largely corresponded those established by visual observations (Fig. 6.3).

6.3 The Stratified Organization of the Inner Plexiform Layer Is Revealed by TNAP Activity in the Rat Retina

The IPL was historically divided into 5 substrata (Cajal 1893; see in Kolb 2007) or in two sublaminae (ON and OFF). Recent electrophysiological studies expanded our knowledge about the functional organization of IPL. Accordingly, it was suggested that the visual world is differentially represented in at least ten parallel strata, thereby creating visual functions such as local edge detection, direction

selectivity and looming detection (Roska and Werblin 2001). Therefore, information about lamina specific pattern of connectivity between retinal cell types in the IPL is pivotal for studies tackling retinal or downward visual processing in the brain.

Roska and Werblin (2001) defined ten IPL strata based on the dendritic arborization and physiological properties of different ganglion cell types in rabbits. Recently, Siegert et al. (2009) divided the mouse IPL into 10 strata by combining starburst amacrine cell marker choline acetyltransferase (ChAT), Ca^{2+} binding protein calretinin (CR), tyrosine hydroxylase (TH; marker of the dopaminergic amacrine cells) and rod bipolar marker protein kinase C alpha subunit (PKCα) immunohistochemical reactions. Notably, the innermost part of the IPL with strong PKCα staining was divided arbitrarily into two strata by the authors.

In rats, we have shown that TNAP histochemistry alone visualized five dark and one fainter TNAP positive strata in the IPL that were separated by thin TNAP negative stripes. These alternating TNAP-positive and negative layers divided the IPL into eleven sequential strata (Fig. 6.2g). The first four TNAP positive and the three TNAP negative strata in the distal IPL were easily discernible. The four additional TNAP positive and TNAP negative strata in the innermost IPL were not always obvious and could only be clearly separated by detailed mathematical analysis (Kántor et al. 2015). The strata revealed by TNAP histochemistry were numerated 1–11 in the disto-proximal direction of the IPL. In our scheme, strata 1, 3, 5, 7, 9 and 11 were TNAP positive and the intermediate TNAP negative layers were strata 2, 4, 6, 8 and 10. Moreover, we performed a further mathematical model based analysis to quantify the exact position of the above strata. Detailed description of the method can be found in Kántor et al. (2015). Briefly, individual TNAP staining intensity profiles of selected IPL areas were generated using Image J. The individual TNAP profiles were combined to generate a mean TNAP staining profile (Fig. 6.4a). Next, the BIC (Bayesian information criteria) was calculated from N = 1 to 12. The BIC measures the optimality of a model by balancing the fitting error and the model complexity. The minimum of the BIC was obtained at N = 6 indicating that the observed TNAP staining can be modeled best by the sum of 6 individual Gaussian curves. Adjusting the amplitude, center position and width of the Gaussians toward smaller fitting error, the best fitting parameter set of the 6 Gaussians emerged. Notably, the fitted model and the mean TNAP profile almost exactly matched (Fig. 6.4b). As a consequence, the fitted model consisted of 6 darker and 5 lighter TNAP stripes in the IPL. The 6 Gaussian curves had similar amplitudes. TNAP activity was highest in the middle part of the IPL, especially in stratum 7. Thereafter, IPL strata borders were determined as the positions of the inflection points of the fitted Gaussians. The most variable staining was observed at IPL depth encompassing strata 7–10. Therefore, as seen in Fig. 6.3a, b on the mean TNAP intensity curve, peaks corresponding to stratum 5 and 7 as well as 9 and 11 lie close together and the minimum value between them is not pronounced.

In rats we performed TH, ChAT, CR, PKCα immunoreaction combined with TNAP histochemistry in the same retinal specimen to determine whether IPL strata defined by TNAP staining correspond those seen with canonical IPL markers. The

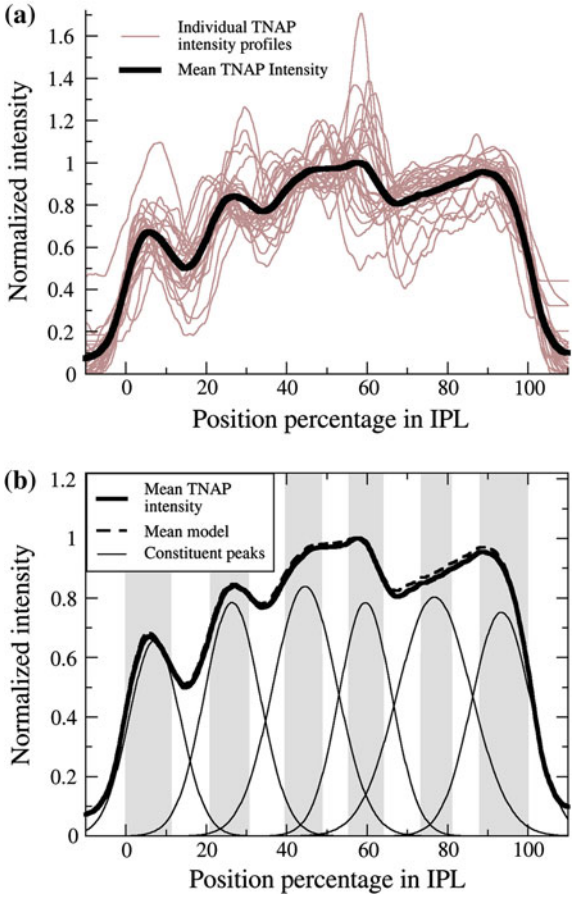

Fig. 6.4 Characterization of TNAP labeled IPL strata in the rat retina using model based analysis. **a** Mean profile of TNAP staining intensity (*dark line* in **a**, **b**) was created from plots of individual TNAP stainings (*light lines*). **b** Using Bayesian information criterion analysis, the best model of the mean TNAP intensity results from the sum of six Gaussian curves (*dotted line* in **b**). Indeed, the best fitting model (*dotted line*) almost exactly matched the mean TNAP intensity profile (*thick line*). Borders of the IPL strata were defined as the inflection points of the Gaussians. According to the model, 11 strata were delineated. Originally published in Cell and Tissue Research, vol. 359, p.415 Fig. 2c,e, Stratified organization and disorganization of inner plexiform layer revelaed by TNAP activity in healthy and diabetic rat retina, Kántor O, Varga A, Tóth R, Énzsöly A, Pálfi E, Kovács-Öller T, Nitschke R, Szél Á, Székely A, Völgyi B, Négyessy L, Somogyvári Z, Lukáts Á. With kind permission from Springer Science and Business media

colocalization of the TNAP strata with that of widely used markers of the IPL is shown in Fig. 6.4a, b. After the images of the above-mentioned different stainings were merged, an exact correspondence of the immunolabeled IPL strata and those labeled by TNAP histochemistry was found (Fig. 6.5a, b). The dark TNAP stratum 1 corresponded to the outermost IPL stratum, which was marked by dendritic

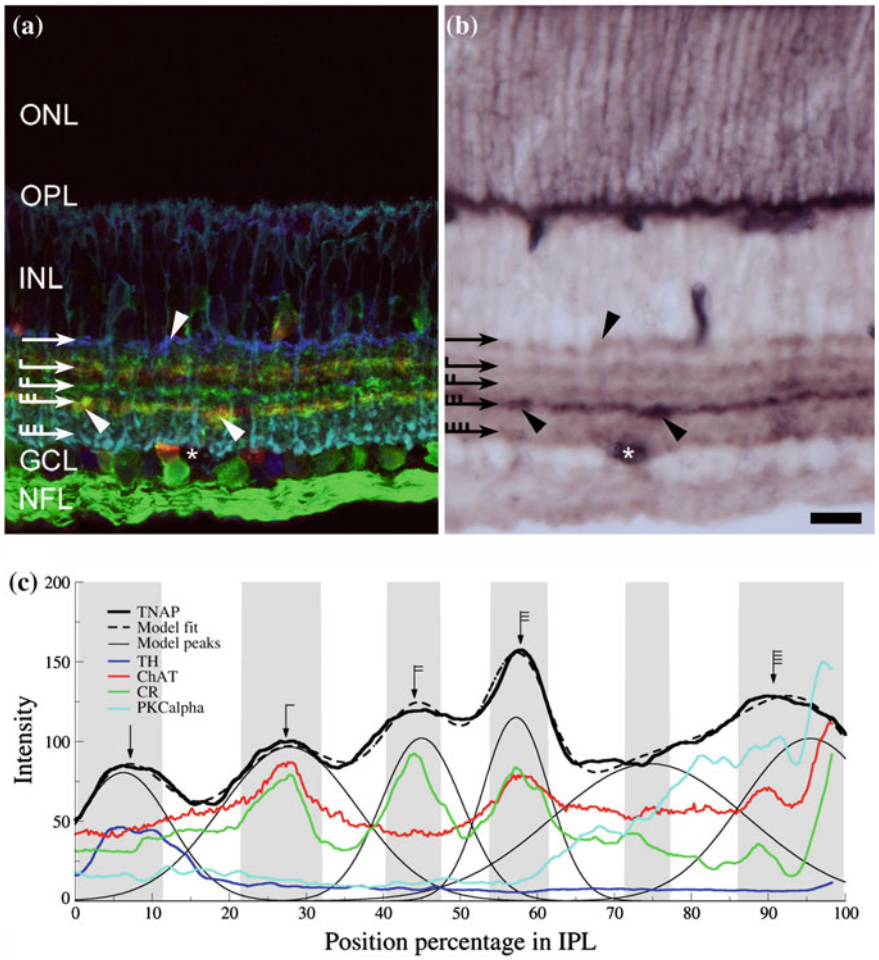

Fig. 6.5 Colocalization of TNAP stained strata of the IPL with canonical markers. Merged confocal image of the quadruple tyrosine hydroxylase (TH, *blue*), choline acetyltransferase (ChAT, *red*), calretinin (CR, *green*) and protein kinase C alpha (PKCα, turquoise) immunohistochemical reactions **a** with TNAP histochemistry **b** on the same specimen revealed the same IPL strata as indicated by the *arrows* (fletched in the same manner). Arrowheads in the same positions indicate corresponding structures in both pictures. Fitting the intensity profiles of the different immunohistochemical stainings (**c**, color coding as in **a**), TNAP histochemistry (*black line*) as well as mean TNAP staining (*dashed line*) showed that the strata revealed by TNAP indeed corresponded to those seen after the combined immunohistochemistry. Strata are depicted as *shaded* and *light* areas. *ONL*: outer nuclear layer, *OPL* outer plexiform layer, *INL* inner nuclear layer, *GCL* ganglion cell layer, *NFL* nerve fiber layer. *Asterisk*: same vessel in **a**, **b**. *Bar* 20 µm. Originally published in Cell and Tissue Research, vol. 359, p. 416 Fig. 3c Stratified organization and disorganization of inner plexiform layer revelaed by TNAP activity in healthy and diabetic rat retina, Kántor O, Varga A, Tóth R, Énzsöly A, Pálfi E, Kovács-Öller T, Nitschke R, Szél Á, Székely A, Völgyi B, Négyessy L, Somogyvári Z, Lukáts Á. With kind permission from Springer Science and Business media

processes of the TH positive amacrine cells. Similarly, dark TNAP strata 3, 5 and 7 exactly matched layers containing CR positive fibers. Strata 3 and 7 were also identified as ChAT positive layers that are generally known to contain dendrites of ON and OFF subpopulations of starburst amacrine cells. In contrast, strata 8–11 lacked all these previous stainings, but all showed strong PKCα labeling. However, the PKCα staining was homogenous and could not clearly delineate strata the way the TNAP staining did. The strongest PKCα labeling, corresponding to the terminals of rod bipolar cells, was observed in the dark TNAP stratum 11. The nine strata of the IPL delineated by the quadruple immunohistochemical reaction exactly corresponded to those seen after TNAP histochemistry alone (Fig. 6.5b). This finding was proven by model fitting analyses of the staining intensity profiles of the different immunolabelings (Fig. 6.5c). In contrast to TH, ChAT, CR, PKCα combined stainings, TNAP histochemistry alone divided the IPL into eleven strata thereby offering a useful alternative to label distinct IPL strata of the rat retina. In addition, with the quadruple immunohistochemical reaction, the innermost part of the IPL was labeled rather homogeneously with PKCα. On the contrary, using TNAP histochemistry alone, it was possible to divide this part of the IPL into three further strata (strata 9–11). Our work demonstrates that TNAP histochemistry is an easy, fast and cost-effective method to visualize the lamination of the rat IPL.

6.4 The Possible Retinal Functions of TNAP—Implications from the Cerebral Cortex

Vitamin B_6 is one of TNAP's substrates (Fedde and Whyte 1990) and serves as a GAD cofactor (Soghomonian and Martin 1998). However, by regulating the level of intracellular pyridoxal phosphate, TNAP can potentially affect other vitamin B_6-dependent enzymes, including those synthesizing glutamate and monoamines (Amadasi et al. 2007). Moreover, functional deficiency in aromatic-L-amino acid decarboxylase enzyme required for the synthesis of dopamine and serotonin has been associated with hypophosphatasia presented by two neonates (Balasubramaniam et al. 2010). Thus, TNAP can affect major neurotransmitter systems in the retina.

Regarding the possible functions, it is important to add the role of TNAP in purinergic signaling via its ectophosphatase activity on all forms (ATP, ADP, AMP) of adenosine phosphates in vitro (Abbracchio et al. 2009; Zhang et al. 2012). Since purinergic receptors are abundant in the retina and purinergic signaling is an important regulator of retinal transmission (Puthussery and Fletcher 2006; Puthussery et al. 2006; Housley et al. 2009) TNAP can possibly influence retinal purinergic signaling.

In vitro, knockdown of TNAP using RNA interference reduced proliferation and differentiation of neural stem cells into either neurons or oligodendrocytes (Kermer et al. 2010). In hippocampal culture blocking of TNAP inhibited the growth and branching of neurons, whereas addition of TNAP promoted axonal growth. TNAP colocalized with $P2X_7$ receptors in the growth cone (Díez-Zaera et al. 2011).

6.5 Possible Involvement of TNAP in Diabetic Retinopathy

In type 1 and type 2 diabetic patients without or with only minimal diabetic retinopathy, significant mitigation of the GCL/IPL was found using optical coherence tomography, whereas no changes in other neural retinal layers were detected, pointing to the early involvement of the inner retina in diabetic retinopathy (van Dijk et al. 2009, 2012). Moreover, visual functions in patients with minimal diabetic retinopathy, such as contrast and color sensitivity, are also disturbed (Ismail and Whitaker 1998; Adams and Bearse 2012).

As part of posttranslational modifications, TNAP isoenzymes became glycosylated. Removal of the N-linked sugar chains resulted in a full loss of enzymatic activity (Nosjean et al. 1997) indicating that altered states of protein glycosylation, as seen in diabetes, might affect TNAP activity. Furthermore, in a large, multiethnic population study, in non-diabetic patients with hyperinsulinemia and insulin resistance, elevated level of bone-type TNAP activity was found (Cheung et al. 2013). Similarly, in vitro, TNAP expression was elevated in an osteoblast cell line in the presence of high glucose and insulin concentrations (Cunha et al. 2014). Conversely, in a streptozotocin-induced rat model of type I diabetes, reduced TNAP activity was found in bone marrow stromal cells (Zhao et al. 2013).

In addition to research on retinal connectomics, TNAP histochemistry can also be useful to investigate the effects of diabetic retinopathy in rat models. In streptozotocin treated rats, 12 weeks after the induction of diabetes, we found an overall reduction of TNAP activity in all retinal layers (Fig. 6.6c). Moreover, in the IPL of diabetic animals, we observed diminished TNAP activity in a patchy pattern, which is in contrast to the continuous activity of the enzyme alongside this layer seen in the control rats (Kántor et al. 2015). This observation indicates that in diabetes, retinal TNAP activity shows regional impairments whereby affected areas are surrounded by regions with apparently preserved TNAP function. The stratified pattern of TNAP staining in the IPL was severely disrupted (46 % overall decrease) in diabetic animals, whereas no change in the stratification pattern of ChAT and CR labeled processes was detected.

Using our model fitting analysis, in diabetic animals, a significant decrease of TNAP activity was found at depths of 5–65 % (corresponding to TNAP strata 1–7) and at 88–100 % (corresponding to stratum 11) of the IPL (Fig. 6.6e, f). No significant difference was found between 65–88 % depth, corresponding to strata 8–10. Moreover, this reduced TNAP activity was also accompanied by a significant drop in the global retinal TNAP mRNA level. The corresponding quantitative PCR reaction revealed a significant reduction of TNAP mRNA in the retina of diabetic animals to 31 % of the control level. The extent of loss is comparable to the results of Zhao et al. (2013), who found a drop of TNAP mRNA level to 39 % of the control in bone marrow stromal cells in streptozotocin induced diabetic rats. This indicates that the reduced TNAP activity is due to (at least partially) the reduced TNAP expression in the retina.

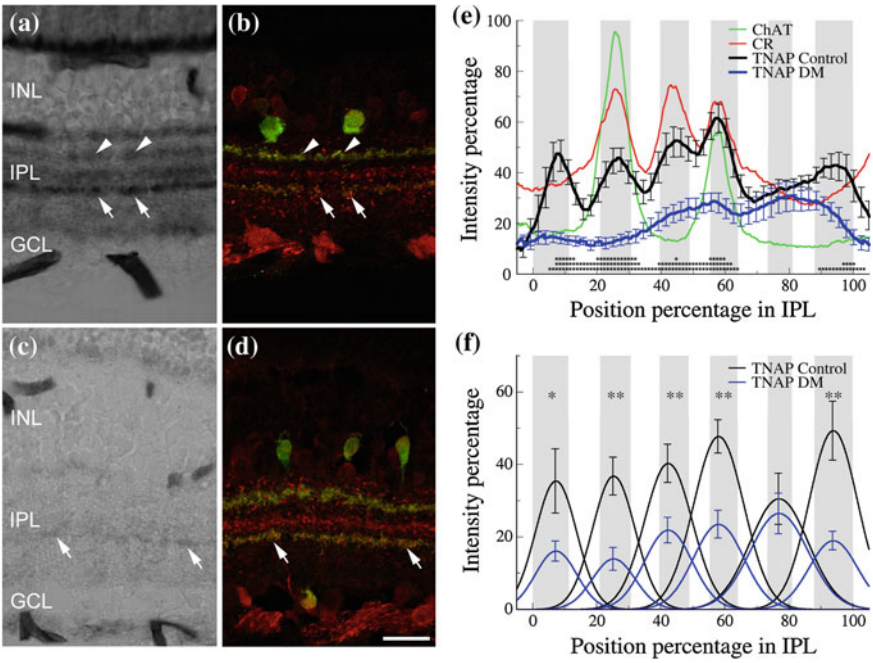

Fig. 6.6 Loss of TNAP activity in the IPL of diabetic rats. Representative confocal images from healthy control **a**, **b** and diabetic rats **c**, **d** depicting TNAP activity **a**, **c** as well as calretinin (CR, *red*) and choline acetyltransferase (ChAT, *green*) immunoreactivities **b**, **d** in the IPL. In diabetic animals, TNAP activity in the IPL was severely diminished, and IPL strata were not discernible. However, no changes in the CR and ChAT stratification patterns were detected at this stage of the disease. **e** Quantitative comparison of the percentage of mean TNAP staining intensity profiles and TNAP positive layers represented by Gaussians **f** between control (n = 7, *black line*/Gaussians) and diabetic retinas (n = 9, *blue line*/Gaussians). The intensity values are normalized to the staining intensity of the vessels in the same photograph. Note that significant decreases were found at the depth of 5–65 % (corresponding to TNAP layers 1–7, that is Gaussians 1–4) and 89–100 % (layer 11, 6th Gaussian) of the IPL. *Error bars* represent SEM values. *Stars* along the X axis represents the significance of the difference at any given position: 1, 2 and 3 *stars* (in vertical orientation) indicate p = 0.05; 0.01 and 0.001 significance levels, respectively *INL* inner nuclear layer, *IPL* inner plexiform layer, *GCL* ganglion cell layer. *DM* diabetes mellitus. *Arrows* and *arrowheads* indicate identical elements of the *IPL*. *Bar* 20 µm. Originally published in Cell and Tissue Research, vol. 359, p. 418 Fig. 5, Stratified organization and disorganization of inner plexiform layer revelaed by TNAP activity in healthy and diabetic rat retina, Kántor O, Varga A, Tóth R, Énzsöly A, Pálfi E, Kovács-Öller T, Nitschke R, Szél Á, Székely A, Völgyi B, Négyessy L, Somogyvári Z, Lukáts Á. With kind permission from Springer Science and Business media

6.6 Possible Role of TNAP in Retinal Development (Review of the Literature)

TNAP′s role in the retinal development is rather scarcely investigated. In chicken embryo, intraocular administration of levamisole (reversible, non-competitive inhibitor of TNAP) led to disturbances in photoreceptor development, reduction of thickness of the OPL and optic fiber layer, reduced number of photoreceptors and degenerating ganglion cells (Araki and Saito 1986; Araki et al. 1987). However, it is yet unknown whether TNAP plays a similar role in retinal development of mammals.

6.7 Retinal Pathology Related to TNAP Functions

In both hypo- and hyperphosphatasia, cases with ophthalmological symptoms can be found in the literature: atypical retinitis pigmentosa was associated to hypophosphatasia (Roxburgh 1983). Kerr et al. (2010) found progressive retinopathy in most of their studied patients (12–14) suffering from primary hyperphosphatasia, sometimes leading even to blindness. The role of phospho-tau protein was implicated in the pathophysiology of glaucoma (Gupta et al. 2008). Since TNAP dephosphorylates hyperphosphorylated tau, a key player in Alzheimer's and in other neurodegenerative diseases (Díaz-Hernandez et al. 2010), TNAP might play a role in the pathophysiology of glaucoma as well. Moreover, recent observations explored retinal neurodegeneration in Alzheimer disease (Guo et al. 2010).

In conclusion, although direct experimental evidence is missing, presence of retinal TNAP activity throughout the vertebrate evolution suggests a fundamental role of this ubiquitous enzyme in visual functions. The present works also summarized the first steps undertaken to reveal TNAP's role in diseases with retinal involvement.

Acknowledgment The work was supported by the Hungarian Scientific Research Fund (OTKA-K113147) to Zoltán Somogyvári.

Conflict of Interest The authors declare no conflict of interest.

References

Abbracchio MP, Burnstock G, Verkhratsky A, Zimmermann H (2009) Purinergic signalling in the nervous system: an overview. Trends Neurosci 32:19–29

Adams AJ, Bearse MA (2012) Retinal neuropathy precedes vasculopathy in diabetes: a function-based opportunity for early treatment intervention? Clin Exp Optom 95:256–265

Amadasi A, Bertoldi M, Contestabile R, Bettati S, Cellini B, di Salvo ML, Borri-Voltattorni C, Bossa F, Mozzarelli A (2007) Pyridoxal 5′-phosphate enzymes as targets for therapeutic agents. Curr Med Chem 14:1291–1324

Araki M, Saito T (1986) Alterations in the differentiation of chick retina caused by an intraocular injection of alkaline phosphatase inhibitor. Exp Eye Res 43:713–728

Araki M, Sato T, Saito T (1987) Effects of alkaline phosphatase inhibitors on chick neural retinal cell differentiation in vitro: ultracytochemical studies. Histochem J 19:579–588

Balasubramaniam S, Bowling F, Carpenter K, Earl J, Chaitow J, Pitt J, Mornet E, Sillence D, Ellaway C (2010) Perintal hypophosphatasia presenting as neonatal epileptic encephalopathy with abnormal neurotransmitter metabolism secondary to reduced co-factor pyridoxal-5′-phosphate availability. J Inherit Metab Dis 33:25–33

Bodis-Wollner I, Miri S, Glazman S (2014) Venturing into the no-man's land of the retina in Parkinsons's disease. Mov Disord 29:15–22

Cajal SR (1893) La retine des vertebres. Cellule 9:119–257

Cheung CL, Tan KC, Lam KS, Cheung BM (2013) The relationship between glucose metabolism, metabolic syndrome, and bone-specific alkaline phosphatase: a structural equation modeling approach. J Clin Endocrinol Metab 98:3856–3863

Cunha JS, Ferreira VM, Maquigussa E, Naves MA, Boim MA (2014) Effects of high glucose and high insulin concentrations on osteoblast function in vitro. Cell Tissue Res 358:249–256

De Vincentiis M, Testa M (1959) Distribution of alkaline and acid phosphatase in the particulate fractions of the retina. J Histochem Cytochem 7:393–394

Dehabadi MH, Davis BM, Wong TK, Cordeiro MF (2014) Retinal manifestations of Alzheimer's disease. Neurodegener Dis Manag 4:241–252

Díaz-Hernandez M, Gómez-Ramos A, Rubio A, Gómez-Villafuertes R, Naranjo JR, Miras-Portugal MT, Avila J (2010) Tissue-nonspecific alkaline phosphatase promotes the neurotoxicity effect of extracellular tau. J Biol Chem 285:32539–32548

Díez-Zaera M, Díaz-Hernández JI, Hernández-Álvarez E, Zimmermann H, Díez-Hernández M, Miras-Portugal MT (2011) Tissue-nonspecific alkaline phosphatase promotes axonal growth of hippocampal neurons. Mol Biol Cell 22:1014–1024

Fedde KN, Whyte MP (1990) Alkaline phosphatase (tissue-nonspecific isoenzyme) is a phosphoethanolamine and pyridoxal-5′-phosphate ectophosphatase: normal and hypophosphatasia fibroblast study. Am J Hum Genet 47:767–775

Fonta C, Négyessy L, Renaud L, Barone P (2004) Areal and subcellular localization of the ubiquitous alkaline phosphatase in the primate cerebral cortex: evidence for a role in neurotransmission. Cereb Cortex 14:595–604

Guo L, Duggan J, Cordeiro MF (2010) Alzheimer's disease and retinal neurodegeneration. Curr Alzheimer Res 7:3–14

Gupta N, Fong J, Ang LC, Yücel YH (2008) Retinal tau pathology in human glaucomas. Can J of Ophthamol 43:53–60

Housley GD, Bringmann A, Reichenbach A (2009) Purinergic signaling in special senses. TINS 32:128–141

Iandiev I, Wurm A, Pannicke T, Wiedemann P, Reichenbach A, Robson SC, Zimmermann H, Bringmann A (2007) Ectonucleotidases in Müller glial cells of the rodent retina: Involvement in inhibition of osmotic cell swelling. Purinergic Signal 3:423–433

Ismail GM, Whitaker D (1998) Early detection of changes in visual function in diabetes mellitus. Ophthalmic Physiol Opt 18:3–12

Kántor O, Varga A, Kovács-Öller T, Énzsöly A, Balogh L, Baksa G, Szepessy Z, Fonta C, Szél Á, Négyessy L, Völgyi B, Lukáts Á (2014) TNAP activity is localized at critical sites of retinal neurotransmission across various vertebrate species. Cell Tissue Res 358:85–98

Kántor O, Varga A, Tóth R, Énzsöly A, Pálfi E, Kovács-Öller T, Nitschke R, Szél Á, Székely A, Völgyi B, Négyessy L, Somogyvári Z, Lukáts Á (2015) The stratified organization and disorganization of the inner plexiform layer revealed by TNAP activity in healthy and diabetic rat retina. Cell Tissue Res 359:409–421

Kermer V, Ritter M, Albuquerque B, Leib C, Stanke M, Zimmermann H (2010) Knockdown of tissue non-specific alkaline phosphatase impairs neural stem cell proliferation and differentiation. Neurosci Lett 485:208–211

Kerr NM, Cassinelli HR, DiMeglio LA, Tau C, Tüysüz B, Cundy T, Vincent AL (2010) Ocular manifestations of juvenile Paget disease. Arch Ophthalmol 128:698–703

Kolb H (2007) Roles of amacrine cells. In: Kolb H, Fernandez E, Nelson R (eds) Webvision: the organization of the retina and visual system (Internet). University of Utah Health Sciences Center, Salt Lake City (UT)

Le Du MH, Millán JL (2002) Structural evidence of functional divergence in human alkaline phosphatases. J Biol Chem 277:49808–49814

Lindeman VF (1949) Alkaline and acide phosphatase activity of the embryonic chick retina. Proc Soc Exp Biol Med 71:435–437

Lutty GA, McLeod DS (2005) Phosphatase enzyme for studying vascular hierarchy, pathology, and endothelial dysfunction in retina and choroid. Vision Res 45:3504–3511

Négyessy L, Xiao J, Kántor O, Kovács GG, Palkovits M, Dóczi TP, Renaud L, Baksa G, Glasz T, Ashaber M, Barone P, Fonta C (2011) Layer-specific activity of tissue non-specific alkaline phosphatase in the human neocortex. Neuroscience 172:406–418

Nosjean O, Koyama I, Goseki M, Roux B, Komoda T (1997) Human tissue non-specific alkaline phosphatases: sugar-moiety-induced enzymic and antigenic modulations and genetic aspects. Biochem J 321:297–303

Puthussery T, Fletcher EL (2006) $P2X_2$ receptors on ganglion and amacrine cells in cone pathways of the rat retina. J Comp Neurol 496:595–609

Puthussery T, Yee P, Vingrys AJ, Fletcher EL (2006) Evidence for the involvement of purinergic $P2X_7$ receptors in outer retinal processing. Eur J Neurosci 24:7–19

Reis JL (1954) Histochemical localization of alkaline phosphatase in the retina. Br J Ophthalmol 38:35–38

Rogers KT (1963) Studies on chick brain differentiation V. Comparative histochemical alkaline phosphatase studies on chick retina, and blackbird, mouse, rabbit, cat and human brains. J Exp Zool 153:21–35

Roska B, Werblin F (2001) Vertical interactions across ten parallel, stacked representations in the mammalian retina. Nature 410:583–587

Roxburgh ST (1983) Atypical retinitis pigmentosa with hypophosphatasia. Trans Ophthalmol Soc UK 103:513–516

Siegert S, Gross Scherf B, Del Punta K, Didlovsky N, Heintz N, Roska B (2009) Genetic address book for retinal cell types. Nat Neurosci 12:1197–1206

Soghomonian JJ, Martin DL (1998) Two isoforms of glutamate decarboxylase: why? Trends Pharmacol Sci 19:500–505

van Dijk HW, Kok PHB, Garvin M, Sonka M, DeVries JH, Michels RPJ, van Velthoven MEJ, Schlingemann RO, Verbraak FD, Abramoff MD (2009) Selective loss of inner retinal layer thickness in type 1 diabetic patients with minimal diabetic retinopathy. IOVS 50:3404–3409. doi:10.1167/iovs.08-3143

van Dijk HW, Verbraak FD, Kok PH, Stehouver M, Garvin MK, Sonka M, DeVries JH, Schlingemann RO, Abramoff MD (2012) Early neurodegeneration in the retina of type 2 diabetic patients. IOVS 53:2715–2719. doi:10.1167/iovs.11-8997

Yoshida M (1957) The alkaline phosphatase activities in the isolated nuclei of ox retina. Jpn J Physiol 7:190–198

Zhang D, Xiong W, Chu S, Sun C, Albensi BC, Parkinson FE (2012) Inhibition of hippocampal synaptic activity by hypoxia or oxygen-glucose deprivation does not require CD73. PLoS ONE 7:e39772

Zhao YF, Zeng DL, Xia LG, Zhang SM, Jiang XQ, Zhang FQ (2013) Osteogenic potential of bone stromal cells derived from streptozotocin-induced diabetic rats. Int J Mol Med 31:614–620